

ON THE APPEARANCE OF MIXED DYNAMICS AS A RESULT OF COLLISION OF STRANGE ATTRACTORS AND REPELLERS IN REVERSIBLE SYSTEMS

A. O. Kazakov*

UDC 517.925+517.93

In this work, we propose a scenario of appearance of mixed dynamics in reversible two-dimensional diffeomorphisms. A jump-like increase in the sizes of the strange attractor and strange repeller, which is due to the heteroclinic intersections of the invariant manifolds of the saddle points belonging to the attractor and the repeller, is the key point of the scenario. Such heteroclinic intersections appear immediately after the collisions of the strange attractor and the strange repeller with the boundaries of their attraction and repulsion basins, respectively, after which the attractor and the repeller intersect. Then the dissipative chaotic dynamics related to the existence of the mutually separable strange attractor and strange repeller immediately becomes mixed when the attractor and the repeller are essentially inseparable. The possibility of realizing the proposed scenario is demonstrated using a well-known problem of the rigid-body dynamics, namely, the nonholonomic model of the Suslov top.

1. INTRODUCTION

Until recently, it has generally been recognized that there are two types of chaos in the finite-dimensional smooth dynamical systems, namely, conservative (e.g., Hamiltonian) chaos and dissipative chaos (strange attractors). Conservative chaos appears in nonintegrable systems having the property of conserving the phase volume, while dissipative chaos is observed in systems whose phase volume is subject to compression and/or expansion during the system evolution. According to the well-known Conley theorem [1], each dynamical system, which is specified on a compact manifold, has an attractor and a repeller. Many various definitions of an attractor are known. In this work, the attractor of the system is understood as a stable (with respect to the constantly acting perturbations) closed invariant manifold, while the repeller is an attractor for the system in inverse time. This definition of an attractor dates back to the works by Conley [1], Ruelle [2], and Hurley [3] and was discussed in detail in recent work [4] (see the definition of a complete attractor in Sec. 2.3.).

It is noteworthy that these definitions of an attractor and a repeller are in perfect agreement with the results of numerical experiments and allow one to determine the third type of dynamic chaos, i.e., mixed dynamics. Therefore, if we denote an attractor and a repeller as \mathcal{A} and \mathcal{R} , respectively, the conditions $\mathcal{A} = \mathcal{R}$ and $\mathcal{A} \cap \mathcal{R} = \emptyset$ are fulfilled for conservative chaos and dissipative chaos, respectively. For the mixed dynamics, an attractor always intersects but does not coincide with a repeller, i.e., the relationships $\mathcal{A} \cap \mathcal{R} \neq \emptyset$ and $\mathcal{A} \neq \mathcal{R}$ [4] are fulfilled.

For the first time, the possibility of intersection of the attractor and the repeller was discovered in [5], in which the following statement was proved. Near a nonrough heteroclinic contour of any two-dimensional

* kazakovdz@yandex.ru

diffeomorphism having two saddle points with the Jacobians greater and smaller than unity¹ there exist open regions (the so-called Newhouse regions) in which the diffeomorphisms with countable sets of asymptotically stable, quite unstable, and saddle periodic orbits, whose closures have nonempty intersections, are dense, which actually means that the attractors and the repellers are inseparable. Later in [6], an analogous theorem was proved for the case where the diffeomorphism f with a circumscribed heteroclinic contour is reversible, i.e., where f and f^{-1} are conjugated using a certain involution h for which $h \circ h = \text{id}$. However, as distinct from the general case, there also appear symmetric periodic orbits of the conservative type (with the Jacobian $J = 1$), such as elliptic and saddle periodic orbits with the multipliers μ and $1/\mu$, apart from the periodic sources and sinks.

According to [7], the symmetric periodic orbits are the periodic orbits which intersect the set $\text{Fix}(h) \cup \text{Fix}(f \circ h)$ exactly at two points. Here, $\text{Fix}(h)$ and $\text{Fix}(f \circ h)$ are sets of fixed points of the involutions h and $f \circ h$, respectively. The symmetric periodic points of the odd period have one point of intersection with the set $\text{Fix}(h)$ and one point of intersection with the set $\text{Fix}(f \circ h)$, whereas the symmetric periodic points of the even period may not intersect the set $\text{Fix}(h)$ at all.

Note that the coexistence of dissipative and conservative dynamics was discovered in papers [8–10], in which it was noted that the phase space for reversible two-dimensional diffeomorphisms can be divided into invariant regions with conservative dynamics where the entire region is a chain transitive set (see the definition of chain transitivity in, e.g., [11]),² and invariant regions containing the attractor–repeller pairs. As far as the attractor–repeller intersection in the physical systems is concerned, numerical experiments confirmed such a possibility (presumably, for the first time) in paper [12] in which it was noted that the attractor and the repeller can overlap. Later in [13], such a behavior in the above-mentioned model was attributed to the appearance of mixed dynamics in the system. Among the studies of mixed dynamics in the models appearing in various applications, one should emphasize the works dedicated to investigating the nonholonomic models of the Celtic stone [14], Chaplygin rubber top [15], Suslov top [16], and Chaplygin sleigh [17, 18], as well as work [19], in which the mixed dynamics was revealed in a model of two vortices under the action of the wave disturbance.

As is shown in [13] by an example of a model of two coupled rotators, mixed dynamics in reversible systems can appear softly and hardly from conservative and dissipative dynamics, respectively. In the former case, the transition from conservative dynamics is accompanied by a sequence of local [7] and global [6, 20] symmetry-breaking bifurcations. In the latter case, mixed dynamics appears explosively after the disappearance (crisis) of the attractor (stable fixed point) and the repeller (quite unstable fixed point).

In this work, we propose a new scenario of the mixed-dynamics appearance in the one-parameter families of two-dimensional reversible diffeomorphisms. In this scenario, the disappearance (crisis) of the chaotic Hénon attractor and the chaotic Hénon repeller, which results from heteroclinic bifurcations, is the key point. In this case, transition to mixed dynamics within the framework of this scenario is realized in a chainlike manner, i.e., as conservative chaos \rightarrow strange attractor + strange repeller \rightarrow mixed dynamics. This scenario is the development of the scenario proposed in [19]. The nonholonomic Suslov model [21] is considered as an example of the problem in which mixed dynamics is realized by this scenario.

This work is organized as follows. In Sec. 2, a brief description of the appearance and the crisis of the Hénon attractor is given using the well-known two-dimensional Hénon map [22] as an example, and the Hénon-attractor properties are considered. Section 3 describes the proposed scenario of the mixed-dynamics appearance in the one-parameter families of two-dimensional reversible maps. Section 4 shows the realization of the proposed scenario by an example of the nonholonomic Suslov model.

¹ Recall that a nonrough heteroclinic contour is a separatrix contour with two saddle points, in which one separatrix pair intersects transversally, while the other one forms the heteroclinic nonrough tangency.

² The inseparable sets of the stable and quite unstable periodic orbits seem to coexist inside such invariant regions. However, since the Jacobians of such orbits are very close to unity, the dynamics in such regions looks like conservative during the numerical simulation.

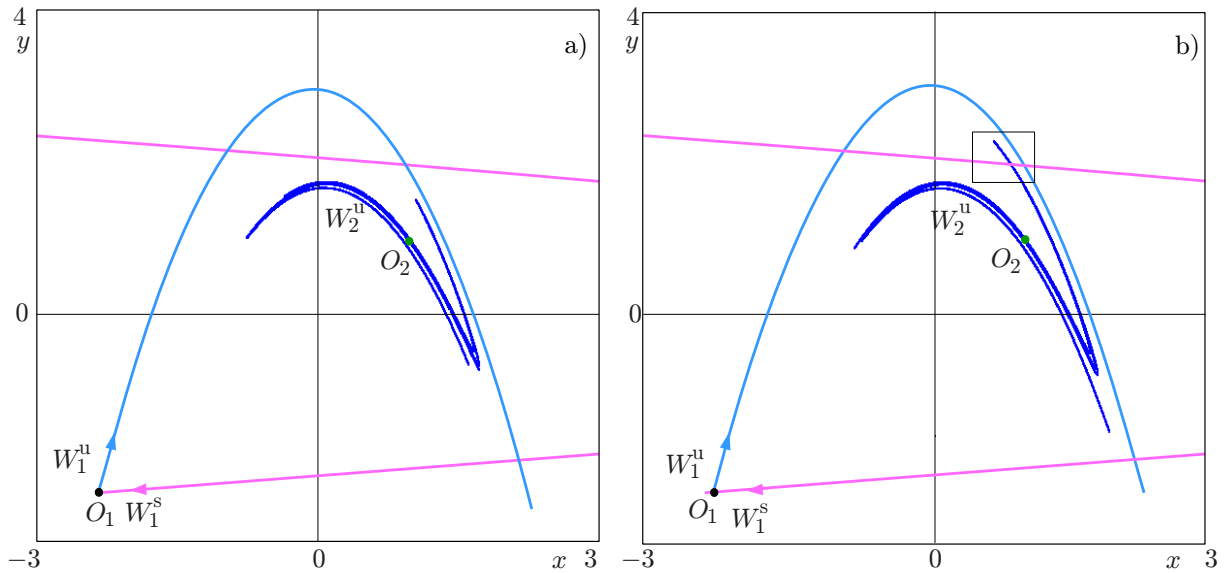


Fig. 1. Collision of the Hénon attractor in map (1) with the attraction-basin boundary for $b = 0.4$ and $M = 2.25$ (a) and $M = 2.27$ (b).

2. HÉNON ATTRACTORS AND THEIR CRISIS

To gain a better understanding of bifurcations leading to collisions between an attractor and a repeller, we consider a scenario of appearance and disappearance (crisis) of an attractor in the Hénon map

$$\bar{x} = y, \quad \bar{y} = M - bx - y^2, \quad (1)$$

where x and y are the map variables, and M and b are the parameters. In [22], it was numerically shown that a strange attractor can appear in the above-mentioned map for some parameters. Then, we take the fixed parameter $b = 0.4$ and describe the scenario of appearance and disappearance of this attractor in the considered map by increasing the parameter M .

For $M \approx -0.485$, the system undergoes a saddle-node bifurcation after which the saddle point O_1 and the stable point O_2 appear. As the parameter M increases, starting from $M \approx 1.47$, the stable point O_2 undergoes a cascade of period-doubling bifurcations, as a result of which a Feigenbaum-like strange attractor [23] appears for $M \approx 2.1825$.

According to the numerical-study results, immediately after the appearance of chaotic dynamics via the cascade of period-doubling bifurcations, the Feigenbaum-like attractor consists of a set of segments (components). As the M parameter continues to increase, the attractor components merge pairwise (as a result of appearance of heteroclinic intersections among the manifolds of saddle periodic points, which belong to the attractor components, and the manifolds of saddle points located between these components). Two components separated by the fixed saddle point, which appeared from the stable point O_2 after the first period-doubling bifurcation, merge last and the homoclinic Hénon attractor is formed. Such an attractor is called homoclinic since after the merging of the two last components this attractor belongs to the closure of the unstable manifold W_2^u of the saddle point O_2 , i.e., contains this saddle point. In this case, it can be assumed that the Hénon attractor is formed by the unstable manifold W_2^u of the point O_2 .

Stable and unstable manifolds are divided by the saddle point into two coupled components, which are called separatrices for convenience in what follows. Then the stable separatrices of the saddle point O_1 are denoted W_1^s and W_2^s .

Note that the attraction basin of the attractor in the Hénon map is bounded by the stable separatrix W_1^s of the saddle point O_1 (see Fig. 1a). As the parameter M continues to increase, the Hénon attractor increases, approaches the separatrix W_1^s , and disappears at $M \approx 2.27$ because of the appearance of hetero-

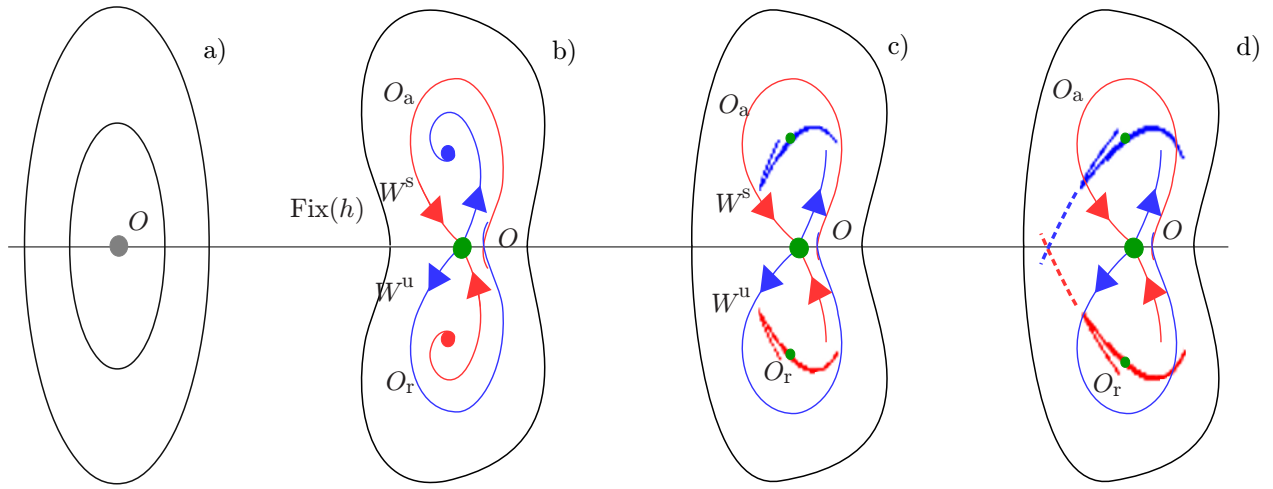


Fig. 2. Scenario of appearance of mixed dynamics as a result of disappearance of the Hénon-like attractor and the Hénon-like repeller.

clinic intersection between W_2^u and W_1^s (see Fig. 1b). In this case, almost all the trajectories from its vicinity go to infinity.

It should be noted that the described scenario of appearance and disappearance of the strange attractor is one of the main scenarios of transition to chaos in dissipative systems. The attractors appearing according to this scenario are called the Hénon-like attractors. As is shown below, the realization of the described scenario in reversible systems can lead to the appearance of another type of chaos, namely, mixed dynamics.

3. SCENARIO OF APPEARANCE OF MIXED DYNAMICS IN REVERSIBLE SYSTEMS

Let us consider an one-parameter family of two-dimensional reversible diffeomorphisms $\bar{X} = F(X, \varepsilon)$ which are specified on compact manifold. Let for $\varepsilon_0 < \varepsilon < \varepsilon_1$, one of fixed points O of the reversible diffeomorphism lie on the line $\text{Fix}(h)$ of the fixed points and be elliptic (see Fig. 2a). Then it is assumed that for $\varepsilon = \varepsilon_1$, the point O undergoes a symmetry-breaking bifurcation [7] as a result of which for $\varepsilon > \varepsilon_1$ this point becomes a symmetric saddle point in whose vicinity the asymptotically stable point O_a and the quite unstable point O_r appear with the same periods as that of the point O . In this case, one unstable separatrix of the saddle point O goes to the sink O_a , one stable separatrix exits from the source O_r , and another separatrix pair, $W^u(O)$ and $W^s(O)$, forms a transversal intersection (see Fig. 2b). With the further increase in the parameter ε , exactly for $\varepsilon = \varepsilon_2$, the Hénon-like attractor AH appears as a result of the scenario described in Sec. 2. In the same manner, the quite unstable point O_r gives birth to the Hénon-like repeller RH.

Note that the basin of attraction of the attractor AH is bounded by the stable manifold $W^s(O)$ of the symmetric saddle point O as in the case of an attractor in the two-dimensional Hénon map. With respect to involution, the repulsion basin of the repeller RH is bounded by the unstable manifold $W^u(O)$. With the further increase in the parameter ε , the attractor AH approaches the boundary of its attraction basin. By analogy, the repeller RH approaches the manifold $W^u(O)$ (see Fig. 2c).

Then it is assumed that for $\varepsilon > \varepsilon_3$, the unstable manifold $W^u(O_a)$, which forms the attractor AH, intersects with the stable manifold $W^s(O)$, i.e., the Hénon-like attractor collides with the boundary of its basin of attraction and disappears. At the same time, the Hénon-like repeller RH disappears as a result of intersection of the manifolds $W^s(O_r)$ and $W^u(O)$. It is important to note that in this case, the separatrices $W^u(O)$ and $W^s(O)$ intersect transversally, as before. Therefore, for $\varepsilon > \varepsilon_3$, one can observe a transversal intersection between the manifolds $W^u(O_a)$ and $W^s(O_r)$ (see Fig. 2d). Thus, as a result of the crisis, the

attractor AH and the repeller RH of the system considerably increase in size and intersect with each other, i.e., mixed dynamics appears.³

4. COLLISION OF THE ATTRACTOR AND THE REPELLER IN THE NONHOLONOMIC SUSLOV MODEL

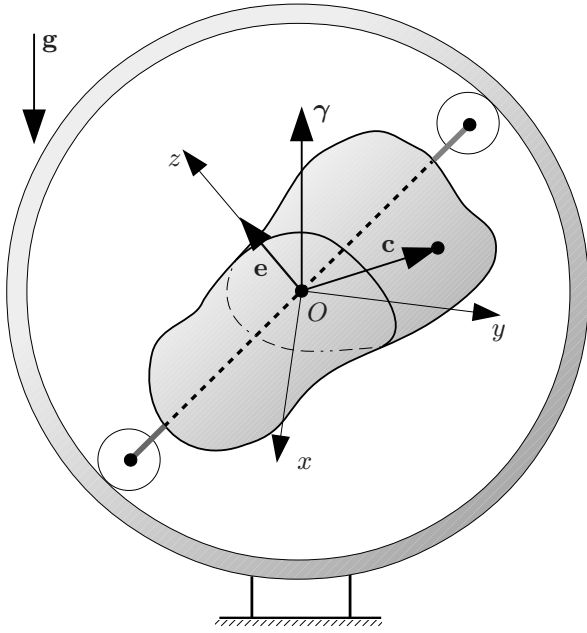


Fig. 3. Suslov constraint realization [25].

Let the origin O be located at the motionless point of the body, the axis Oz be collinear with the vector \mathbf{e} that is motionless in the body, and the axes Ox and Oz be directed so as to bring to zero the inertia-tensor elements I_{12} and, correspondingly, I_{21} (see Fig. 3). Then, the nonholonomic constraint $(\boldsymbol{\omega}, \mathbf{e}) = 0$ takes the simple form $\omega_3 = 0$. In this case, the system of equations determining the angular velocity $\boldsymbol{\omega} = (\omega_1, \omega_2, 0)$ and the orientation $\boldsymbol{\gamma} = (\gamma_1, \gamma_2, \gamma_3)$ of the top, where $\gamma_1, \gamma_2,$ and γ_3 are the projections of the vertical vector $\boldsymbol{\gamma}$ onto the axes $Ox, Oy,$ and Oz , respectively, is determined as follows [21]:

$$\begin{aligned} I_{11}\dot{\omega}_1 &= -\omega_2(I_{13}\omega_1 + I_{23}\omega_2) - mgc_3\gamma_2 + mgc_2\gamma_3, \\ I_{22}\dot{\omega}_2 &= \omega_1(I_{13}\omega_1 + I_{23}\omega_2) - mgc_1\gamma_3 + mgc_3\gamma_1, \\ \dot{\gamma}_1 &= -\gamma_3\omega_2, \quad \dot{\gamma}_2 = \gamma_3\omega_1, \quad \dot{\gamma}_3 = \gamma_1\omega_2 - \gamma_2\omega_1. \end{aligned} \quad (2)$$

Here, $I_{11}, I_{22}, I_{13},$ and I_{23} are the nonzero elements of the inertia tensor of the body, m is the top mass, g is the gravitational acceleration, the vector $\mathbf{c} = (c_1, c_2, c_3)$ specifies the displacement of the center of mass of the top with respect to the sphere center O (see Fig. 3), and the dot denotes the time derivative.

The above-written system of equations possesses the energy and geometric integrals

$$E = \frac{1}{2}(I_{11}\omega_1^2 + I_{22}\omega_2^2) - mg(\mathbf{c} \cdot \boldsymbol{\gamma}) = \text{const}, \quad G = (\boldsymbol{\gamma} \cdot \boldsymbol{\gamma}) = \text{const}. \quad (3)$$

The values of the geometric integral are always fixed, such that $G = 1$ and the value of the energy integral $E = h$ is considered as another parameter in the system. With allowance for integrals (3), equations (2)

As an example of the model in which the above-considered scenario is realized, we consider the system describing the motion of the Suslov top, i.e., a heavy rigid body with a motionless point, which is subject to the nonholonomic constraint specified by the equality of the scalar product $(\boldsymbol{\omega} \cdot \mathbf{e})$ to zero [21]. Here, $\boldsymbol{\omega} = (\omega_1, \omega_2, \omega_3)$ is the angular-velocity vector of the top and \mathbf{e} is the unit vector which is motionless in the body. Therefore, during the motion of the Suslov top, its angular-velocity projection onto a certain motionless axis in the body is equal to zero. Such a constraint was introduced in [24].

As an instructive example of the model in which the described constraint is naturally realized, let us mention the structure proposed in [25], in which a rigid body with a motionless point rolls on sharp wheels inside a motionless sphere (see Fig. 3). The sharp edges of the wheels prevent the body from moving in the direction that is normal to their plane.

Let us choose a coordinate system $Oxyz$, which is rigidly connected with the body in the following manner.

³By analogy, one can observe the crisis (disappearance) of the attractor in the Hénon map [22]. However, in this case, after the attractor intersection with the stable separatrix, which bounds the attraction basin of the attractor, almost all the trajectories go to infinity.

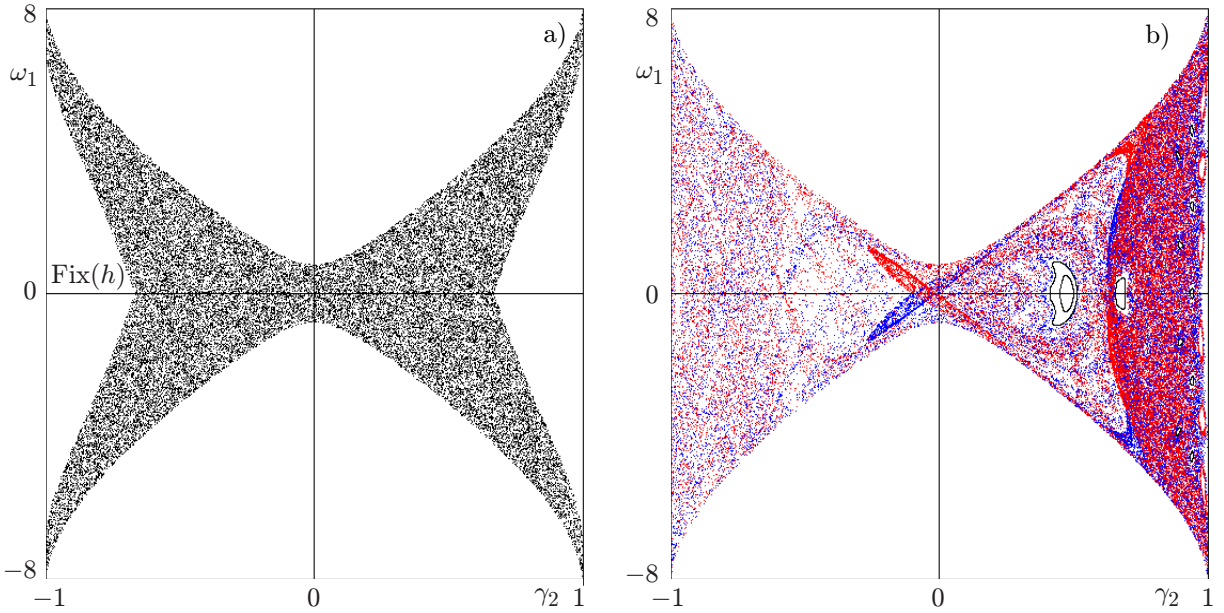


Fig. 4. Conservative chaos for $I_{23} = 0$ (a) and mixed dynamics for $I_{23} = 0.908$ (b). The blue and red dots correspond to the attractor and the repeller, respectively.

specify the three-dimensional flow on a certain compact three-dimensional manifold. To parametrize this flow, by analogy with [21], we use the variables γ_2, ω_1 , and γ_1 , expressing ω_2 and γ_3 in terms of integrals (3). Then, choosing $\gamma_1 = \text{const}$ as the secant, we obtain the two-dimensional Poincaré map

$$(\bar{\gamma}_2, \bar{\omega}_1) = P(\gamma_2, \omega_1). \quad (4)$$

Everywhere below, when performing numerical experiments, we fix the parameters

$$h = 101, m = 1, g = 10, I_{11} = 3, I_{22} = 4, I_{13} = 0, c_1 = 0, c_2 = 0, c_3 = 10 \quad (5)$$

and vary the parameter I_{23} .

Note that for these parameters, system (2) is reversible with respect to involution:

$$H : \{\omega_1 \rightarrow -\omega_1, \quad \gamma_1 \rightarrow -\gamma_1, \quad t \rightarrow -t\}.$$

Therefore, if we choose $\gamma_1 = 0$ as a secant plane, then this involution yields the involution

$$h : \{\omega_1 \rightarrow -\omega_1\}$$

on the two-dimensional Poincaré map (4), and the set of fixed points $\text{Fix}(h)$ of the obtained involution is given by the straight line

$$\text{Fix}(h) = \{\omega_1 = 0\}.$$

4.1. Numerical results

In what follows, we vary the parameter I_{23} , assuming that all other parameters are specified in accordance with conditions (5). For $I_{23} = I_{13} = 0$, as it was shown in [26], a smooth invariant measure exists in the system, i.e., chaos observed in the numerical experiments (see Fig. 4a) is conservative (in the sense that the entire phase space is a chain transitive set).

The case $I_{23} > 0$ was considered in detail in [21], in which one can observe asymmetry between the attractor and the repeller (see Fig. 4b). In [16], such asymmetry was related to the mixed-dynamics

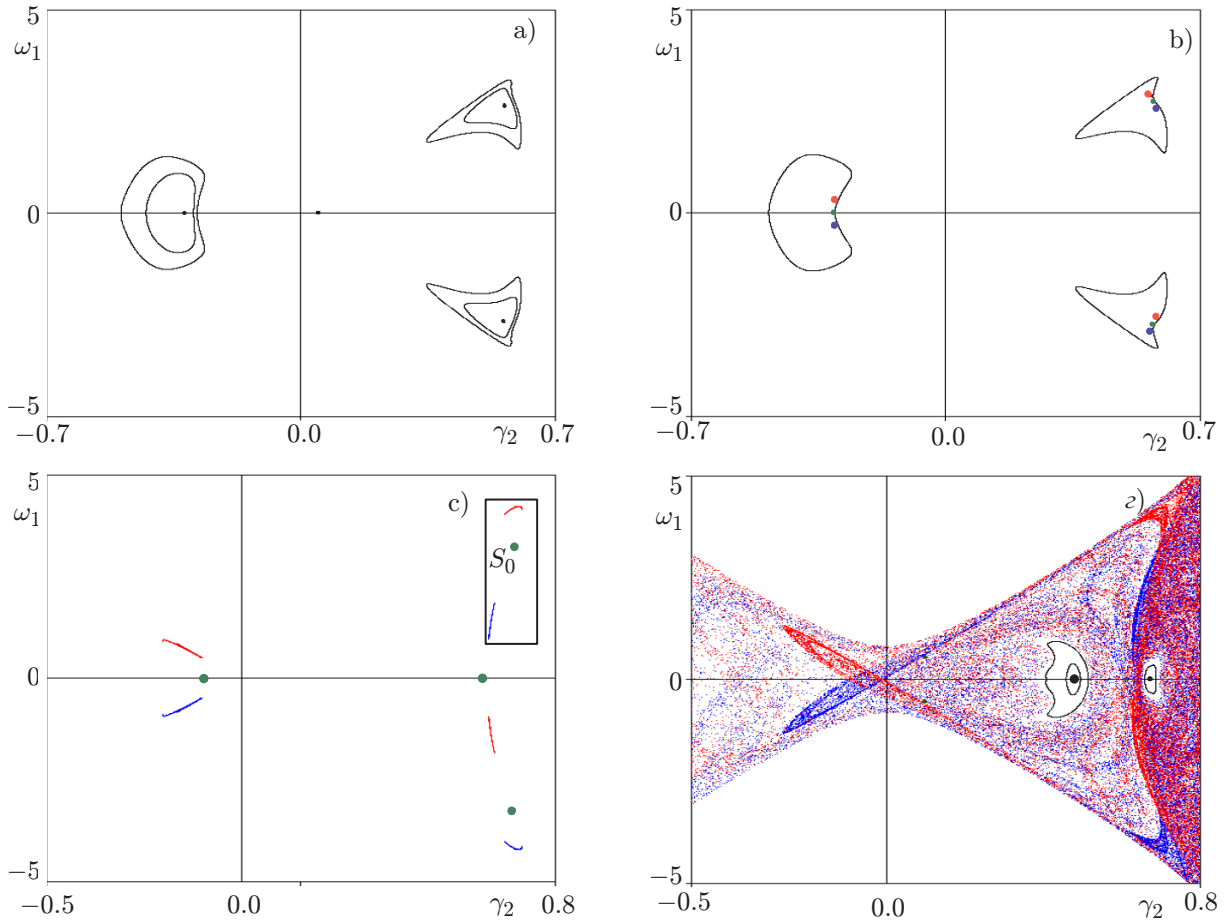


Fig. 5. Scenario of appearance of mixed dynamics in the nonholonomic Suslov model for $I_{23} = 0.7800$ (a), 0.7840 (b), 0.9078 (c), and 0.9080 (d).

appearance in the system. In what follows, we describe in detail the scenario resulting in a transition from conservative chaos to the mixed dynamics with increasing parameter I_{23} .

For $I_{23} = 0.692$, a symmetric elliptic point of period 3 (see Fig. 5a) appears in the system. Then, for $I_{23} = 0.7835$, this elliptic point is subject to the symmetry-breaking bifurcation and eventually becomes the saddle point (S_0), in whose vicinity the asymptotically stable and quite unstable points of period 3 appear (see Fig. 5b). With the further increase in the parameter I_{23} , the Hénon-like attractor and repeller appear from the stable periodic point and the quite unstable point, respectively (see Fig. 5c).

It is noteworthy that the studied system is monostable in the considered parameter range, i.e., the Hénon-like attractor and the Hénon-like repeller are global in the system. Then, for $I_{23} = 0.9079$, the attractor and the repeller disappear according to the scenario described in Sec. 3. The attractor, which appears after that, intersects with the repeller, and the mixed dynamics, which is shown in Fig. 5d, appears.

Let us describe in more detail the homoclinic bifurcations leading to the appearance of mixed dynamics in the considered system. Figure 6 shows the location of the stable (W_o^s) and unstable (W_o^u) separatrices of the symmetric saddle point S_0 , which appears after the symmetry-breaking bifurcation, as well as the unstable separatrix W_a^u , which forms the Hénon attractor, and the stable separatrix W_r^s forming the Hénon repeller. For $I_{23} < 0.9079$, the stable separatrix W_o^s and the separatrix W_o^u bound the attraction and repulsion basins of the Hénon attractor and repeller, respectively (see Fig. 6a). For $I_{23} > 0.9079$, the unstable manifold W_a^u , which forms the attractor, intersects with the separatrix W_o^s , whereas the manifold W_r^s , which forms the repeller, intersects with W_o^u . In this case, since the second pair of the separatrices of the saddle point S_0 already intersects transversally (which is not shown in the figure), intersection between the sepa-

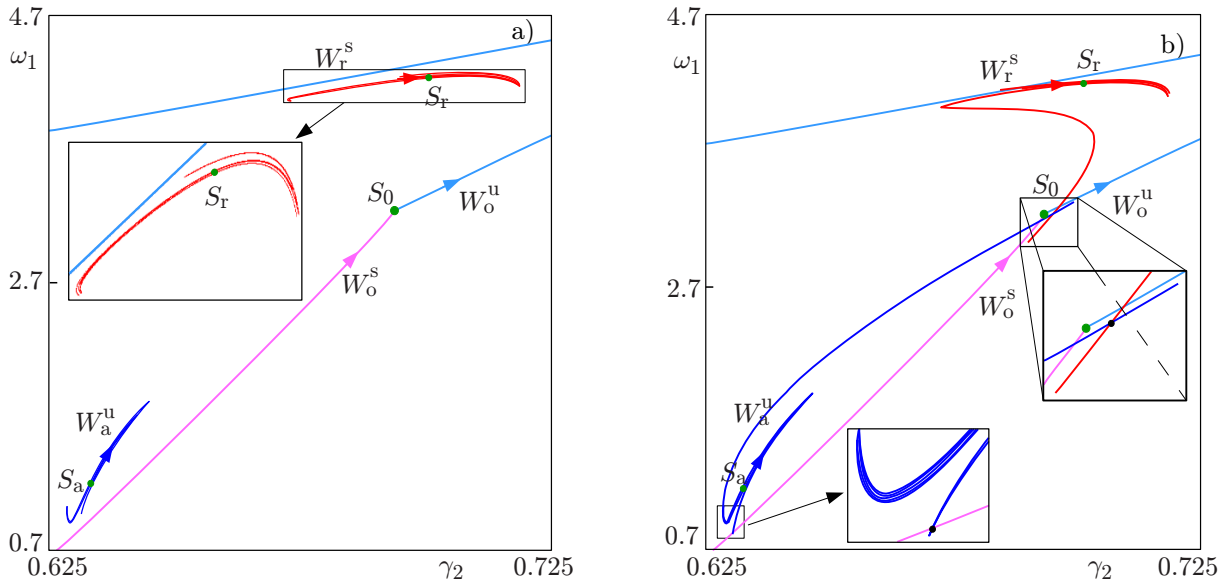


Fig. 6. Homoclinic bifurcations leading to the appearance of the mixed dynamics for $I_{23} = 0.9078$ (a) and $I_{23} = 0.9080$ (b).

matrices W_a^u and W_r^s appears immediately (see Fig. 6b). Therefore, the system attractor appearing after the Hénon-attractor disappearance intersects with the repeller, and mixed dynamics, which is shown in Fig. 5d, is formed.

5. CONCLUSIONS

In this work, we have proposed a new bifurcation scenario of the explosive appearance of mixed dynamics. Within the framework of the considered scenario, the separated Hénon-like attractor and repeller undergo a crisis after which the strange attractor of the system immediately intersects with the strange repeller.

It has been shown that mixed dynamics in the nonholonomic model of the Suslov top appears in full correspondence with the proposed scenario. Moreover, we assume that such a scenario can also be observed in many other reversible systems demonstrating mixed dynamics.

Sections 3 and 4 of this work were supported by the Russian Science Foundation (project No. 17-11-01041). Section 2 was performed within the framework of the Program for Fundamental Studies of National Research University “Higher School of Economics” in 2018 and with support of the Russian Foundation for Basic Research (project No. 18-31-20052).

REFERENCES

1. C. Conley, in: *CBMS Regional Conf. Series in Mathematics, Vol. 38*, American Mathematical Society, Providence, RI (1978), p. 89.
2. D. Ruelle, *Commun. Math. Phys.*, **82**, No. 1, 137 (1981).
3. M. Hurley, *Trans. Am. Math. Soc.*, **269**, No. 1, 247 (1982).
4. S. V. Gonchenko and D. V. Turaev, in: *Proc. V. A. Steklov Math. Inst. Rus. Acad. Sci.*, **297**, 133 (2017).
5. S. V. Gonchenko, D. V. Turaev, and L. P. Shil’nikov, in: *Proc. V. A. Steklov Math. Inst. Rus. Acad. Sci.*, **216**, 76 (1997).
6. J. S. W. Lamb and O. V. Stenkin, *Nonlinearity*, **17**, No. 4, 1217 (2004).

7. L. M. Lerman and D. Turaev, *Regul. Chaot. Dyn.*, **17**, Nos. 3–4, 318 (2012).
8. A. Politi, G. L. Oppo, and R. Badii, *Phys. Rev. A*, **33**, No. 6, 4055 (1986).
9. J. A. G. Roberts and G. R. W. Quispel, *Phys. Rep.*, **216**, Nos. 2–3, 63 (1992).
10. J. S. W. Lamb and J. A. G. Roberts, *Physica D*, **112**, No. 1, 1 (1998).
11. D. V. Anosov and I. U. Bronshtein, “Smooth dynamical systems, Ch. 3, Topologic dynamics,” in: *Itogi Nauki Tekhn., Ser. Probl. Mat. Fund. Napr.*, **1**, 204 (1985).
12. D. Topaj and A. Pikovsky, *Physica D*, **170**, No. 2, 118 (2002).
13. A. S. Gonchenko, S. V. Gonchenko, A. O. Kazakov, and D. V. Turaev, *Physica D*, **350**, 45 (2017).
14. A. S. Gonchenko, S. V. Gonchenko, and A. O. Kazakov, *Regul. Chaot. Dyn.*, **18**, No. 5, 521 (2013).
15. A. O. Kazakov, *Regul. Chaot. Dyn.*, **18**, No. 5, 508 (2013).
16. A. Kazakov, in: *Dynamics, Bifurcations and Chaos 2015 (DBC II): Extended Abstract of Int. Conf. and School, Nizhny Novgorod, July 20–24, 2015*, p. 21.
17. S. P. Kuznetsov, *Europhys. Lett.*, **118**, No. 1, 10007 (2017).
18. S. P. Kuznetsov, *Regul. Chaot. Dyn.*, **23**, No. 2, 178 (2018).
19. A. O. Kazakov, *arXiv:1801.00150 [math.DS]* (2017).
20. A. Delshams, S. V. Gonchenko, V. S. Gonchenko, et al., *Nonlinearity*, **26**, No. 1, 1 (2012).
21. I. A. Bizyaev, A. V. Borisov, and A. O. Kazakov, *Regul. Chaot. Dyn.*, **20**, No. 5, 605 (2015).
22. M. Hénon, *The Theory of Chaotic Attractors*, Springer, New York (1976).
23. M. J. Feigenbaum, *Physica D*, **7**, Nos. 1–3, 16 (1983).
24. G. K. Suslov, *Theoretical Mechanics* [in Russian], Gostekhizdat, Moscow–Leningrad (1946).
25. V. V. Vagner, in: *Proc. Workshop on Vector and Tensor Analysis*, No. 5, 301 (1941).
26. V. V. Kozlov, *Usp. Mekh.*, **8**, No. 3, 85 (1985).